MTOC translocation modulates IS formation and controls sustained T cell signaling

Noa B. Martín-Cófreces,[1] Javier Robles-Valero,[1] J. Román Cabrero,[1] María Mittelbrunn,[1,2] Mónica Gordón-Alonso,[1] Ching-Hwa Sung,[3] Balbino Alarcón,[4] Jesús Vázquez,[4] and Francisco Sánchez-Madrid[1,2]

[1]Servicio de Inmunología, Hospital de la Princesa, Universidad Autónoma de Madrid, 28006 Madrid, Spain
[2]Fundación Centro Nacional de Investigaciones Cardiovasculares, 28029 Madrid, Spain
[3]Dyson Vision Research Institute, Weill Medical College of Cornell University, New York, NY 10021
[4]Centro de Biología Molecular Severo Ochoa, Consejo Superior de Investigaciones Científicas, Universidad Autónoma de Madrid, Cantoblanco, 28049 Madrid, Spain

The translocation of the microtubule-organizing center (MTOC) toward the nascent immune synapse (IS) is an early step in lymphocyte activation initiated by T cell receptor (TCR) signaling. The molecular mechanisms that control the physical movement of the lymphocyte MTOC remain largely unknown. We have studied the role of the dynein–dynactin complex, a microtubule-based molecular motor, in the process of T cell activation during T cell antigen–presenting cell cognate immune interactions. Impairment of dynein–dynactin complex activity, either by overexpressing the p50-dynamitin component of dynactin to disrupt the complex or by knocking down dynein heavy chain expression to prevent its formation, inhibited MTOC translocation after TCR antigen priming. This resulted in a strong reduction in the phosphorylation of molecules such as ζ chain–associated protein kinase 70 (ZAP70), linker of activated T cells (LAT), and Vav1; prevented the supply of molecules to the IS from intracellular pools, resulting in a disorganized and dysfunctional IS architecture; and impaired interleukin-2 production. Together, these data reveal MTOC translocation as an important mechanism underlying IS formation and sustained T cell signaling.

Introduction

T cell activation is achieved through the presentation of a specific antigen by an antigen-presenting cell (APC). This process involves the formation of a specialized structure (the immune synapse [IS]) at the T cell–APC contact site. Upon T cell receptor (TCR) activation by antigen recognition, the T cell molecules involved in the formation of the IS reorganize to form this highly segregated structure (Dustin et al., 1998). The TCR and associated molecules congregate in the central area (central supramolecular activation cluster [cSMAC]), whereas adhesion receptors reorganize in a surrounding external ring called the peripheral SMAC (pSMAC; Monks et al., 1998). This differential distribution has been shown to be necessary for full T cell activation (Grakoui et al., 1999) and allows the spatiotemporal regulation of signaling pathways emanating from the IS (Lee et al., 2003). As part of this process, the T cell cytoskeleton reorganizes in order to provide a physical platform to support the IS structure. The actin cytoskeleton forms a ring superimposed on the pSMAC, whereas the tubulin cytoskeleton is vectorially directed toward the center of the IS, where the microtubule-organizing center (MTOC) translocates (Ryser et al., 1982; Kupfer et al., 1987; Kupfer and Singer, 1989). The role of the actin cytoskeleton in T cell activation has been widely studied, and its remodeling upon TCR engagement is required for full T cell activation (Das et al., 2002; Vicente-Manzanares and Sanchez-Madrid, 2004; Billadeau et al., 2007).

The reorganization of the tubulin cytoskeleton has also been found to be important for MTOC translocation and T cell effector functions. The vectorial movement of the MTOC toward the IS is readily observed upon antigen-specific TCR engagement (Sancho et al., 2002b), bringing the secretory apparatus (Golgi) into close apposition to the APC, and thereby

Correspondence to F. Sánchez-Madrid: fsanchez.hlpr@salud.madrid.org

Abbreviation used in this paper: ADAP, adhesion and degranulation promoting adapter protein; APC, antigen-presenting cell; CMAC, 7-amino-4-chloromethylcoumarin; cSMAC, central SMAC; CTL, cytotoxic T lymphocytes; DHC, dynein heavy chain; FN, fibronectin; IL-2, interleukin-2; IS, immune synapse; LAT, linker of activated T cells; LFA-1, lymphocyte function–associated antigen 1; MTOC, microtubule-organizing center; PLL, poly-L-lysine; pSMAC, peripheral SMAC; SEB, *Staphylococcus aureus* enterotoxin B; SEE, *Staphylococcus aureus* enterotoxin E; SMAC, supramolecular activation cluster; TCR, T cell receptor; ZAP70, ζ chain–associated protein kinase 70.

The online version of this paper contains supplemental material.

The Rockefeller University Press $30.00
J. Cell Biol. Vol. 182 No. 5 951–962
www.jcb.org/cgi/doi/10.1083/jcb.200801014

providing the basis for polarized secretion (Kupfer and Dennert, 1984; Kupfer et al., 1991). Moreover, MTOC translocation has been shown to be essential for normal cell function in cytotoxic T lymphocytes' (CTL) killing of target cells (Kupfer et al., 1985). More recently, it has been shown that the secretory granules that contain the effector proteins for cell killing move toward the translocated MTOC, promoting an efficient target clearance by CTL (Stinchcombe et al., 2006). However, to date there have been no published studies providing a clear-cut demonstration of a relationship between MTOC translocation and T cell activation.

Among the candidate signaling molecules involved in MTOC translocation are members of the src tyrosine kinase family such as Lck and Fyn (Lowin-Kropf et al., 1998; Sedwick et al., 1999; Martin-Cofreces et al., 2006). Other signaling and adaptor molecules associated with TCR-specific signaling, such as ζ chain–associated protein kinase 70 (ZAP70), SLP76, and adhesion and degranulation promoting adapter protein (ADAP)/Fyb/SLAP130, are also required for MTOC translocation in T cells (Lowin-Kropf et al., 1998; Blanchard et al., 2002; Barreiro et al., 2007). CD2AP, an adaptor protein essential for CD2 clustering and segregation at the IS, is also necessary for MTOC translocation (Dustin et al., 1998). Interestingly, CD2AP-deficient T cells show deficient segregation of lymphocyte function–associated antigen 1 (LFA-1) and TCR at the IS (Lee et al., 2003).

Despite these advances, the molecular mechanisms that drive MTOC translocation during T cell activation remain largely unknown. Recently, the dynein intermediate chain has been identified as part of a protein complex with ADAP that localizes at the pSMAC in the IS (Combs et al., 2006). Dynein possesses microtubule minus-end motor activity, and multimolecular dynein–dynactin complexes have been implicated in the positioning of the MTOC at the leading edge of migrating fibroblasts and epithelial cells (Palazzo et al., 2001). Full functioning of dynein requires the activity of dynactin (King et al., 2003; Ross et al., 2006). These molecular complexes are linked through the interaction of the p150-glued subunit of dynactin and the p74 dynein intermediate chain (Vaughan and Vallee, 1995). Dynein–dynactin complexes can carry a variety of cargoes by combining different light intermediate chains and light chains. Among the components of this multisubunit complex, the p50-dynamitin subunit can prevent dynein–dynactin complex activity (Hirokawa, 1998; Vaughan, 2005). Recently, in vitro experimentation has revealed that the presence of an excess of exogenous dynamitin leads to the destabilization of the dynactin shoulder structure formed by p150-glued and p24 subunits, which causes their disassembly from dynactin complex (Melkonian et al., 2007). In some cell processes, p50-dynamitin-GFP overexpression might not prevent microtubule minus-end directed movement. This is the case with the intracellular reorientation toward the MTOC of *Chlamydia trachomatis* particles, despite the fact that dynein and dynactin colocalize in nascent *C. trachomatis* inclusions and the movement is dynein dependent (Grieshaber et al., 2003). This effect could be explained by a dynactin-independent dynein function.

We have investigated the role of the dynein–dynactin complex in MTOC translocation upon antigen- and superantigen-driven TCR activation in Jurkat and CH7C17 T cells. Different dynein and dynactin subunits, such as p150 and p74, are enriched at the IS upon stimulation with antigen or superantigen. MTOC translocation was impaired by stable overexpression of a p50-dynamitin-GFP construct or by dynein heavy chain (DHC) silencing. Moreover, expression of p50-dynamitin-GFP altered the segregation of CD3 at the IS central cluster and of LFA-1 at the pSMAC, with subsequent disturbance in the activation of signaling proteins such as ZAP70, linker of activated T cells (LAT), and Vav1. These data highlight the importance of dynein–dynactin complex activity in MTOC translocation and the transduction of TCR signals after antigen stimulation.

Results

Inhibition of dynein–dynactin activity impairs MTOC translocation at the T cell–APC contact area

To study the molecular mechanisms that rearrange the tubulin cytoskeleton and translocate the MTOC to the contact area with the antigen presenting cell, we determined the localization of dynein–dynactin complex components in conjugates formed between two different cell pairs: J77 Jurkat T cells bearing a Vβ8-containing TCR, conjugated to *Staphylococcus aureus* enterotoxin E (SEE)-pulsed Raji APC; and CH7C17 T cells bearing a Vβ3-containing TCR specific for HA peptide, conjugated to HA peptide- or *S. aureus* enterotoxin B (SEB)-pulsed Hom2 APC (not depicted). Cells were labeled with specific antibodies against the p74 dynein subunit, which was mainly enriched at tubulin-based cytoskeletal structures. Similar localization patterns were observed for the p50-dynamitin subunit (Echeverri et al., 1996), and for p150-glued, the component of the dynactin complex that mediates interaction with dynein (Figs. 1 and S1, available at http://www.jcb.org/cgi/content/full/jcb.200801014/DC1; Vaughan and Vallee, 1995).

In most J77-Raji or CH7C17-Hom2 conjugates, the MTOC was located in the contact area between the T cell and the APC (arrows in Fig. 1, A and B; see also the Z maximal projections in Fig. S1, A and B). The components of the dynein–dynactin complex (p150, p50, and p74) were detected at the reoriented MTOC and were highly enriched at the tubulin cytoskeleton localized close to the membrane of the contact area (Fig. 1, A and B; z projections in Fig. S1, A–C), which corresponds with the periphery of the T-APC contact area. We further analyzed the behavior of dynactin components in GFP-Jurkat cells that were conjugated to SEE-pulsed Raji cells and fixed shortly afterward (3 min). Before reorientation of the MTOC, there was an initial clustering of p150-glued and p50-dynamitin subunits at the cell–cell contact area (Fig. S1 C). Subsequently, in cells fixed 20 min after conjugation, major clustering of dynactin subunits was observed at the IS together with MTOC translocation (Fig. S1 C).

To assess whether the dynein–dynactin complex is functionally involved in MTOC reorientation, we generated J77 cell clones that express levels of p50-dynamitin coupled to GFP similar to those of the endogenous protein (Fig. S2, A and B, available at http://www.jcb.org/cgi/content/full/jcb.200801014/DC1). We found that the binding of the dynein p74 intermediate chain

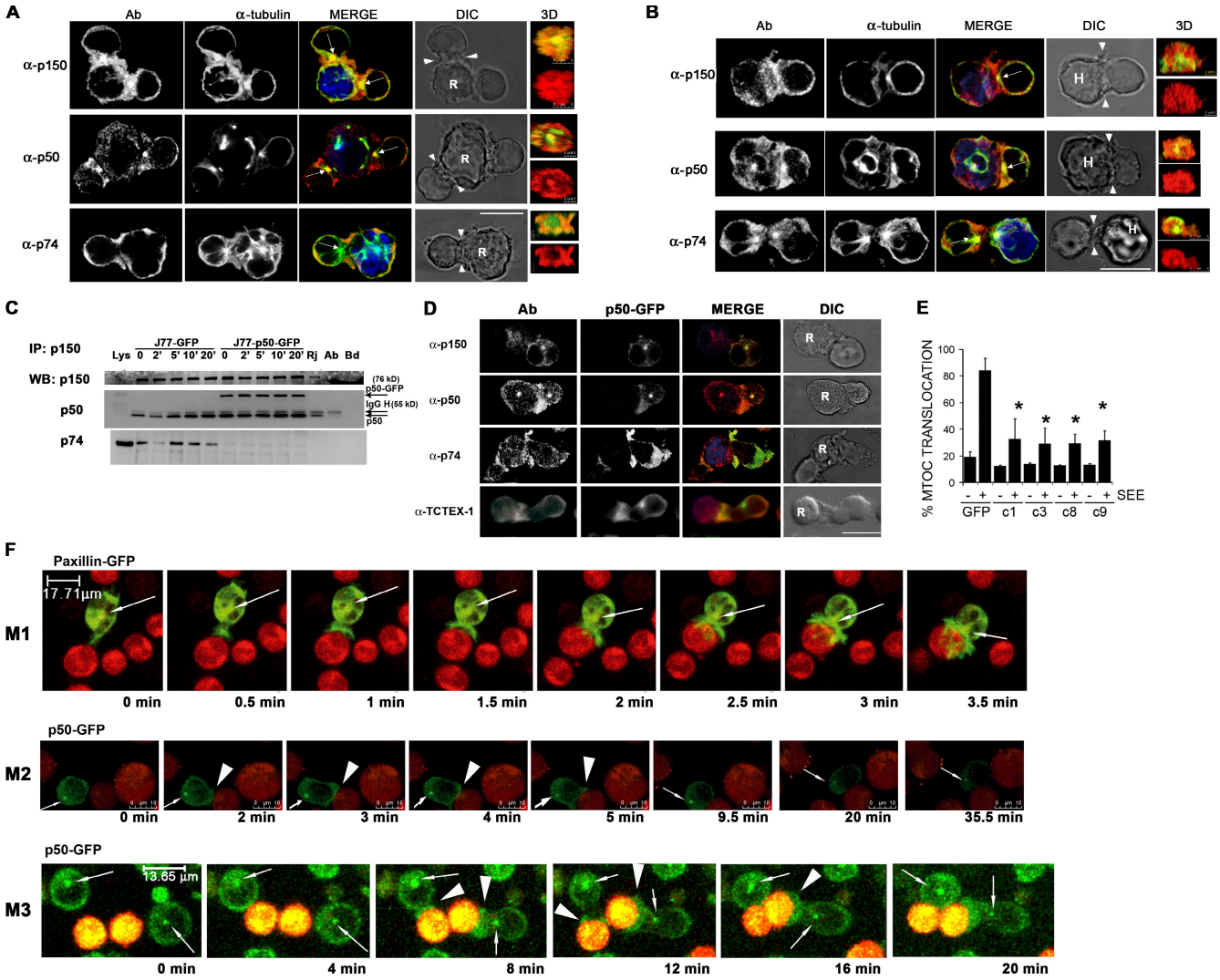

Figure 1. **Overexpression of p50-dynamitin-GFP impairs MTOC translocation upon TCR stimulation.** (A and B) Dynein–dynactin components are found at the contact area between T and APC. The conjugates of J77 Jurkat T cells and SEE-pulsed Raji APC (A) or CH7C17 T cells and HA-pulsed Hom2 APC (B) were fixed with paraformaldehyde. Raji (R) and Hom2 (H) APC were CMAC-labeled (blue). Dynein–dynactin components were detected with specific antibodies (Ab; α-p150, p150-glued; α-p50, p50-dynamitin; α-p74, p74 dynein intermediate chain, clone 74.1) followed by Alexa 568–labeled anti–mouse secondary antibody (red in merged images). α-tubulin was detected with FITC-labeled antibody (green). Confocal z slices and corresponding 3D reconstructions of SMAC area (right) are shown (arrowheads in the z slice mark the cell–cell junction selected for 3D projection; arrows indicate MTOC). Bars, 10 μm. (C) p50-dynamitin-GFP overexpression prevents dynein–dynactin complex formation upon TCR stimulation. p150-glued was immunoprecipitated (IP) from J77 Jurkat cells overexpressing GFP (J77-GFP) or p50-dynamitin-GFP (J77-p50-GFP), then left unstimulated or stimulated by SEE during the indicated times. Samples were processed by Western blotting (WB) using the indicated antibodies. Arrows indicate positions of endogenous (50 kD) and GFP-tagged p50 (76 kD) and IgG H (55 kD). Ab, immunoprecipitating antibody; Bd, G–agarose-coupled beads; Lys, whole lysate; Rj, Raji cells. (D) Dynein–dynactin components cluster at IS in dynamitin-disrupted cells. Conjugates of dynamitin-disrupted Jurkat T cell clones and SEE-pulsed Raji APC (CMAC-labeled, blue) were processed as in A. GFP is shown in green. Bar, 10 μm. (E) Quantification of MTOC translocation in SEE-stimulated dynamitin-disrupted clones (c1, c3, c8, and c9) and GFP control cells. A total of 600 conjugates were counted from five independent experiments. Data are means ± SD. *, $P < 0.05$ versus GFP (Student's *t* test). (F) Time-lapse confocal video microscopy sequence showing the dynamics of MTOC movement in Jurkat cells overexpressing paxillin-GFP (green, control) or p50-dynamitin-GFP (green) at the indicated times. MTOC translocation was stimulated with SEE-pulsed Raji APC loaded with CMCTR cell tracker (red/orange). Images were captured at 37°C. Arrows indicate the position of the MTOC; arrowheads indicate T cell ISs. M, movie.

to dynactin p150-glued in T lymphocytes changes rapidly upon SEE stimulation. There is a transient decrease in this molecular association at short times (0–2 min; Fig. 1 C, J77-GFP), but the binding is recovered shortly after (5–20 min; Fig. 1 C, J77-GFP). Exogenous p50-dynamitin exerted an inhibitory role on the dynein–dynactin complex by preventing the interaction of dynein p74 with the dynactin component p150-glued (Fig. 1 C, J77-p50-GFP). We obtained four dynamitin-disrupted clones, which behaved identically and were used indistinctly in subsequent experiments. Expression of p50-dynamitin-GFP protein (Fig. S2 A) did not interfere with cell viability (unpublished data), and the GFP construct was stable in the cell, showing no sign of degradation as determined by Western blotting (Fig. S2 B). The p50-dynamitin-GFP protein showed a similar distribution to endogenous p50 and p150-glued (Fig. 1 D).

We next assessed the behavior of dynein–dynactin complex components, the MTOC, and the associated Golgi apparatus when the T clones were stimulated with SEE-pulsed Raji cells. In all

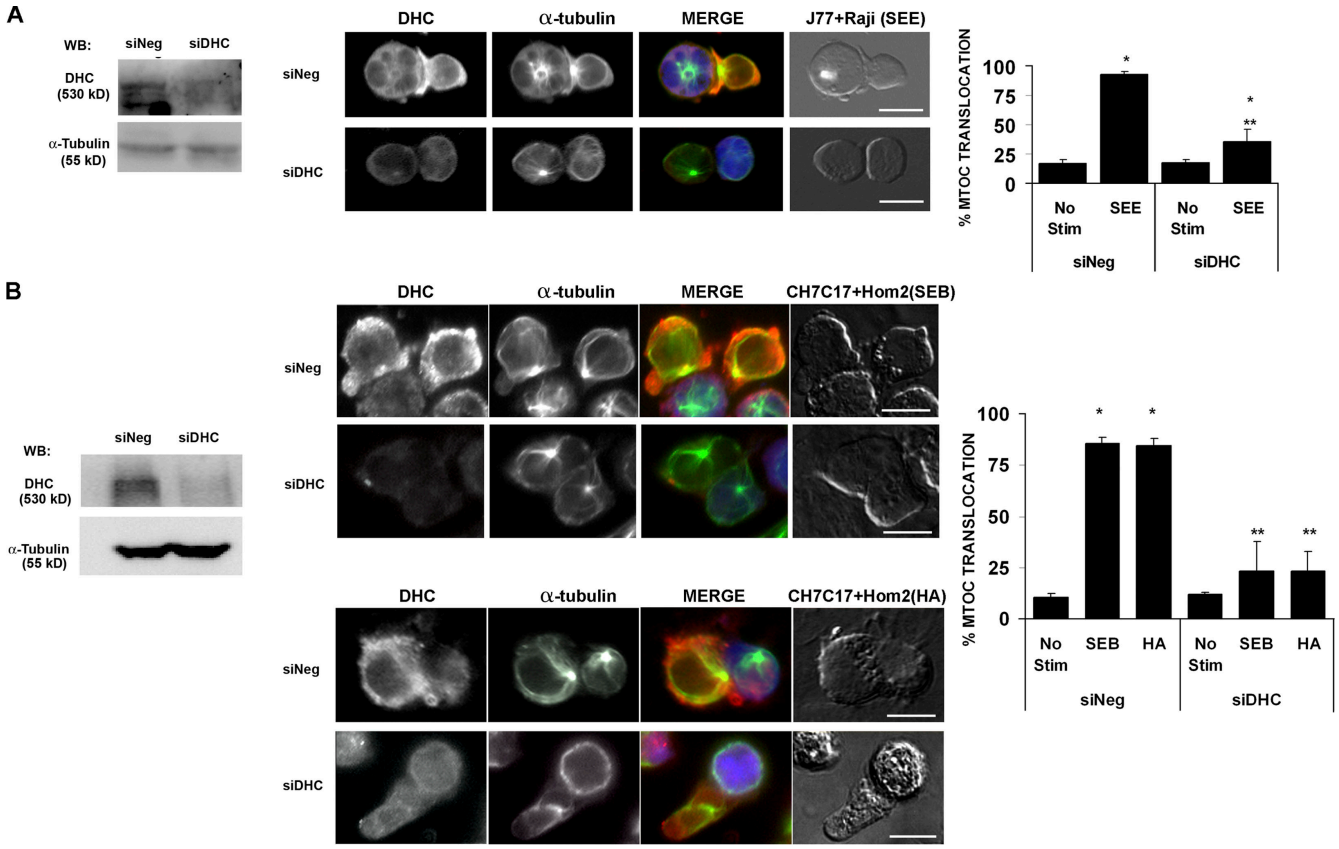

Figure 2. **DHC RNA interference prevents MTOC translocation.** Jurkat cells (A) and CH7C17 cells (B). (left) The effect of DHC siRNA expression (siDHC). DHC was detected by Western blotting with anti-DHC goat polyclonal antibody. (middle) In control cells (siNeg), DHC is localized at the periphery of the IS, surrounding the MTOC. This accumulation does not occur in DHC-interfered cells (siDHC), which fail to translocate their MTOC. Conjugates were formed as in Fig. 1. DHC was detected with anti-DHC clone 440, followed by Alexa 568–labeled anti–mouse secondary antibody (red in the merge image). Tubulin was detected as in Fig. 1 (green). SEE-pulsed Raji and HA or SEB-pulsed Hom2 APC are blue in the merged image (CMAC-labeled). Differential interference contrast images are shown on the right. Bars, 10 μm. (far right) Quantification of MTOC translocation in conjugated Jurkat (A) or CH7C17 (B) T cells. More than 200 conjugates were counted for each condition. Data are means ± SD. *, $P < 0.05$ versus no stimulation; **, $P < 0.001$ versus siNeg (Student's *t* test).

four dynamitin-disrupted clones, MTOC translocation to the contact area with the Raji cell was defective (Fig. 1, D and E). The dynein–dynactin components p150-glued, p74, and TCTEX-1 were localized both at the untranslocated MTOC and at the cell–cell contact area (Fig. 1 D). p50-dynamitin-GFP was also detected at the T cell contact zone, which suggests that the defective MTOC translocation might be the result of a local inhibition of the dynein–dynactin complex (Fig. 1, D and F, arrowheads in M2 and M3; and Videos 2 and 3, available at http://www.jcb.org/cgi/content/full/jcb.200801014/DC1). The impaired MTOC translocation observed in dynamitin-disrupted T cells might be caused by a failure to relocalize toward the APC, or, alternatively, there might be a defect in anchorage once the MTOC reaches the cell-to-cell contact area. To investigate this, we monitored the movement of the MTOC in J77 T cells by time-lapse confocal videomicroscopy, starting from the initial contact with the SEE-prepulsed Raji cells. MTOC movement in the dynamitin-disrupted clones was either random or not evident, showing no effective rearrangement toward the IS (Fig. 1 F, arrows in M2 and M3; and Videos 2 and 3). In contrast, in control cells overexpressing a paxillin-GFP construct (Herreros et al., 2000), the MTOC moved directly to the IS within the first 2–5 min (Fig. 1 F, arrows in M1; and Video 1).

Therefore, in all clones and at all SEE doses, the p50-dynamitin-GFP construct was clustered at the plasma membrane in the T cell contact area with the APC (Fig. 1 D and F, arrowheads in M2 and M3; Videos 2 and 3; and not depicted), which is in accordance with the localization of p74 and p150. However, p74 and p150 interaction was not detected in these conditions. These data strongly support the involvement of the dynactin complex in MTOC translocation, in cooperation with the dynein complex. In correspondence, the Golgi apparatus, which was found to be well-organized around the MTOC in the clones expressing p50-dynamitin-GFP, was not reorientated toward the IS, nor was the MTOC (Fig. S3, available at http://www.jcb.org/cgi/content/full/jcb.200801014/DC1).

Dynein siRNA interference prevents MTOC translocation

To further assess the role of the dynein–dynactin complex in T cell activation, we impaired its nucleation by knocking down the expression of the DHC subunit (530 kD). The DHC is composed of the globular ATPase domains that interact with microtubules and allows the movement of dynein along them (Hirokawa, 1998; Vaughan, 2005). In these experiments, J77 Jurkat and

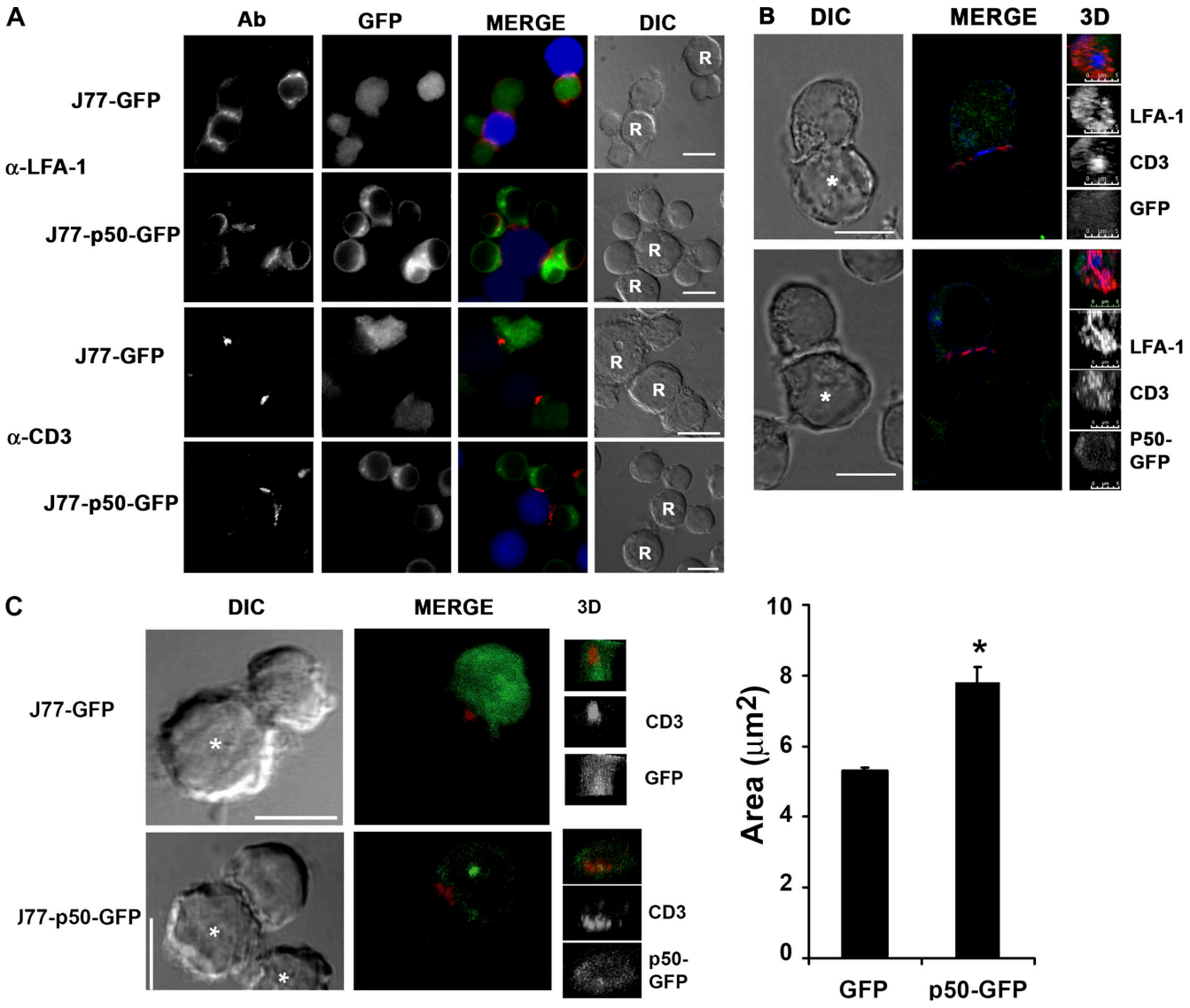

Figure 3. **Dynamitin-disrupted T cells form altered LFA-1 and CD3 clusters at the contact area with the APC.** (A) LFA-1 and CD3 cluster at the IS in dynamitin-disrupted cells. Conjugates between J77 Jurkat control (GFP) or dynamitin-disrupted cells were formed, fixed as in Fig. 1, and stained for LFA-1 or CD3, followed by rhodamine red X–labeled anti–mouse secondary antibody (red in merged images). GFP, green; R, Raji APC (CMAC-labeled, blue). (B) LFA-1 and CD3 show a correct SMAC architecture in control cells (GFP) but not in dynamitin-disrupted cells. A confocal z slice of conjugates formed and processed as in A is shown (3D). LFA-1 is shown in red (Alexa 568–labeled anti–mouse secondary antibody) and CD3 was detected with 448 antibody, followed by an Alexa 647–labeled anti–rabbit secondary antibody (blue). GFP, green. (C) In dynamitin-disrupted clones, CD3 clusters occupy a larger area and appear scattered at the contact area with the APC. A confocal z section of conjugates formed and processed as in A is shown (3D). CD3 was detected with T3b monoclonal antibody followed by rhodamine red X–labeled anti–mouse secondary antibody (red). Asterisks indicate SEE-Raji APC (B and C). (C, right) Quantitative analysis of the CD3-stained area at the IS. Data are means ± SEM. 20 cells were analyzed per condition. *, $P < 0.05$ versus GFP (Student's *t* test). Bars, 10 μm.

CH7C17 T cells were transfected with a combination of two specific DHC siRNA oligonucleotides (siDHC). In both cell types, DHC expression was reduced by 70% with respect to cells expressing control oligonucleotide (siNeg; Fig. 2, A and B). In siNeg-transfected cells, DHC accumulated at the IS around the translocated MTOC (Fig. 2, A and B), as seen for other dynein components (Fig. 1). However, in DHC-interfered cells, although some of the remaining DHC gathered at the IS, this distribution was markedly altered (Fig. 2, A and B). Only 35% of the MTOC were translocated to the IS in DHC-interfered J77 cells stimulated with SEE, representing an inhibition with respect to control cells of >50% (Fig. 2 A). In the case of DHC-interfered CH7C17 cells, the proportions of cells with MTOC translocated toward SEB or HA peptide-loaded APC were, respectively, 23.4 and 23.6% compared with corresponding control values of 85.8 and 84.4% (Fig. 2 B). These data agree with the observed inhibition of MTOC translocation in the J77 clones expressing p50-dynamitin-GFP, and point to a direct role of dynein–dynactin complex activity in MTOC translocation.

p50-dynamitin-GFP overexpression alters SMAC architecture at the IS

We next examined the effect of p50-dynamitin-GFP expression on the organization of the SMAC at the IS, after TCR activation.

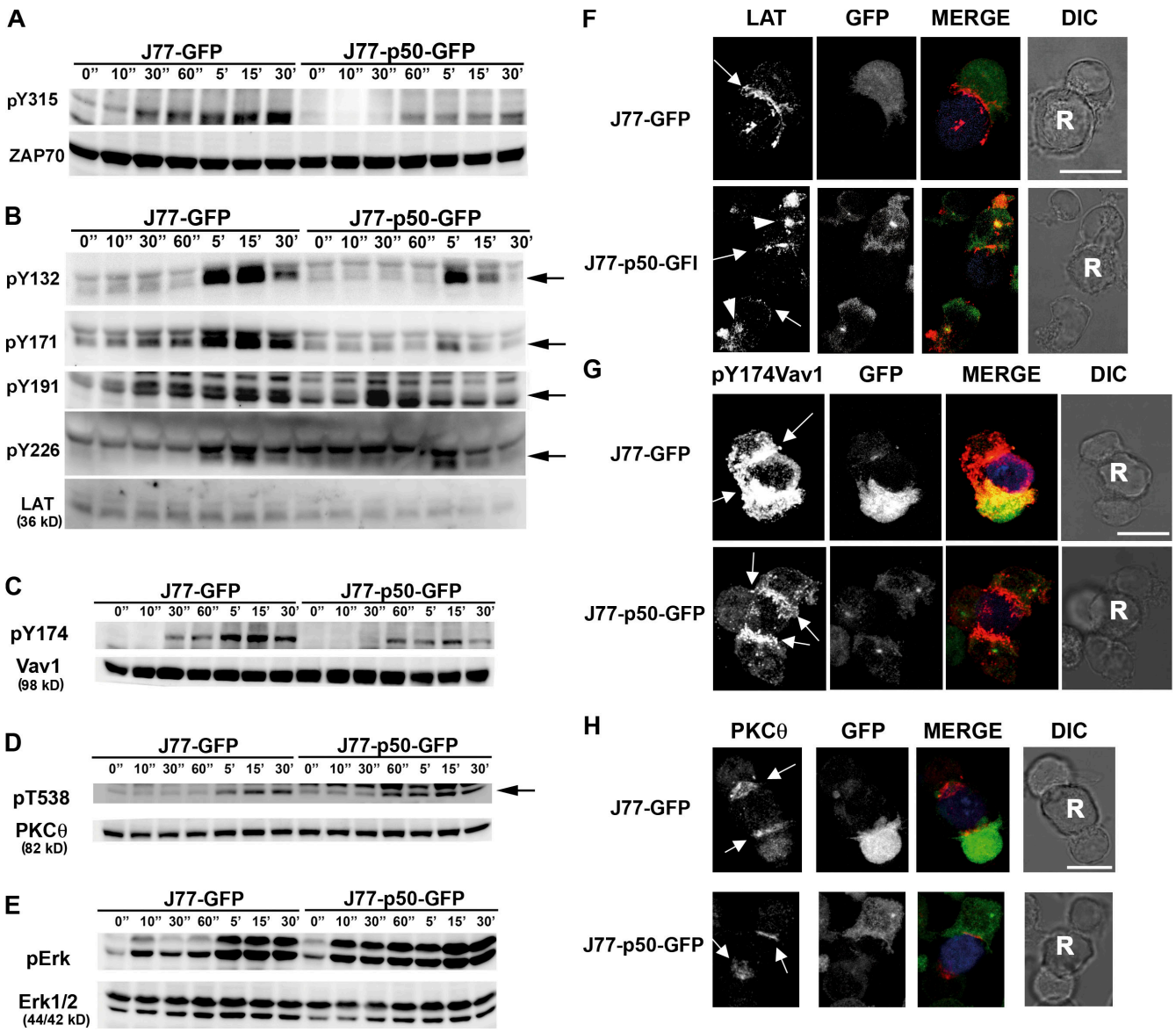

Figure 4. **Overexpression of p50-dynamitin-GFP impairs sustained signaling via the TCR.** (A–E) Western analysis of signaling proteins in J77-GFP or dynamitin-disrupted cells upon stimulation with SEE for the times indicated. Whole lysates were processed for phosphorylated and total protein expression as follows: (A) ZAP70 pY315 and total ZAP70; (B) LAT pY132, pY171, pY191, pY226, and total LAT; (C) Vav1 pY174 and total Vav1; (D) PKCθ pT538 and total PKCθ; and (E) phosphorylated and total Erk1/2, followed by the corresponding HRP-conjugated secondary antibodies. One out of four representative experiments is shown. Arrows indicate target band sizes. (F–H) Conjugates formed and stained for proteins involved in IS formation and maturation (red in merged images, Alexa 568–labeled anti–mouse secondary antibody): LAT (F; arrowheads indicate the fraction of LAT associated with the nontranslocated MTOC in the dynamitin-disrupted clones and not delivered to the nascent IS), pY174Vav1 (G), and PKCθ (H). Arrows indicate the IS area. R, SEE-Raji APC (CMAC-labeled, blue). Bars, 10 μm.

For this purpose, both LFA-1 and CD3 localization were analyzed to assess p- and cSMAC architecture, respectively. LFA-1 integrin clustering was comparable between control J77 T cells and clones expressing p50-dynamitin-GFP (Fig. 3 A), and CD3 molecules were consistently redistributed toward the contact area with the SEE-pulsed Raji APC (Fig. 3 A). Analysis of SMACs showed that LFA-1 integrin was not clearly displaced from the cSMAC in the dynamitin-disrupted clones; this contrasted with control Jurkat cells, in which the characteristic LFA-1 integrin-pSMAC ring was evident (Fig. 3 B). However, the p50-dynamitin-GFP colocalized with ADAP, forming a ring at the IS (Fig. S4, available at http://www.jcb.org/cgi/content/full/jcb.200801014/DC1). This supports the idea that dynein and dynactin are closely associated at the IS and that MTOC movement is functionally linked to ADAP (Combs et al., 2006). Interestingly, confocal 3D reconstruction revealed that CD3 in dynamitin-disrupted T cells was localized in several microclusters near the pSMAC rather than in a central cluster (Fig. 3 C). Quantitative analysis confirmed that this anomalous distribution was associated with an increased CD3 cluster area in dynamitin-disrupted clones (Fig. 3 C, right). The altered CD3 distribution could provoke or instead be a reflection of an alteration in the distribution of activated downstream effectors in the IS. Confirming this, although staining with the anti-phosphotyrosine antibody (4G10) revealed an accumulation

of phosphotyrosine at the IS in transfected control T cells, the clustering of tyrosine phosphorylated proteins in dynamitin-disrupted clones was not as clear cut (Fig. S5).

Inhibition of the dynein–dynactin complex alters sustained signaling downstream of the TCR

The results presented earlier prompted us to study how different signaling pathways are affected by disruption of the dynein–dynactin complex. We next examined the specific phosphorylation of ZAP70, LAT, Vav1, PKCθ, and Erk1/2, molecules known to be important for T cell activation. Phosphorylation of ZAP70 at Y315 was lower in the dynamitin-disrupted clones compared with control cells (Fig. 4 A). This residue functions as a docking site for the SH2 domain of Vav1 and is a marker of T cell activation (Wu et al., 1997). ZAP70 phosphorylates LAT at residue Y191 (Paz et al., 2001), this event being necessary for the scaffolding function of LAT. Phosphorylation of LAT at Y191 in dynamitin-disrupted T cells was observed 10–30 s after SEE stimulation but, in contrast to control cells, was not sustained for longer periods (Fig. 4 B). Consistently, Vav1, which associates with LAT through phospho-Y191 (Paz et al., 2001), showed reduced phosphorylation on Y174 in dynamitin-disrupted T cells (Fig. 4 C), which suggests that the guanine nucleotide exchange activity of Vav1 may be affected in these cells (Lopez-Lago et al., 2000).

Defective tyrosine phosphorylation of other LAT residues (Y132, Y171, and Y226) was also detected in dynamitin-disrupted clones. Once phosphorylated, these tyrosines act as docking sites for specific signaling proteins (Paz et al., 2001), and each shows characteristic activation kinetics (Houtman et al., 2005). Immediate early phosphorylation was consistently detected in the clones; i.e., see Y191-LAT (Fig. 4 B). However, the signal vanished more rapidly in dynamitin-disrupted cells (see phosphorylation of Y191, Y171, Y226, and Y132 after 5 min and beyond; Fig. 4 B). These data suggest that sustained tyrosine phosphorylation induced upon TCR triggering is impaired when MTOC translocation is altered, thereby disrupting the regulation of ZAP70 and LAT phosphorylation upon TCR stimulation. This would affect signaling pathways downstream of LAT, as observed for Vav1 activation (Fig. 4 C). In contrast, phosphorylation of PKCθ at T538 occurred more rapidly in dynamitin-disrupted clones than in control cells (Fig. 4 D), and Erk1/2 phosphorylation was faster and stronger (Fig. 4 E).

LAT from intracellular compartments is not delivered to the IS in cells overexpressing p50-dynamitin-GFP

Several signaling proteins, including LAT, accumulate at the IS of untransfected T cells upon TCR triggering (Blanchard et al., 2002; Bonello et al., 2004). Immunofluorescence analysis showed that LAT was also concentrated at the IS of control cells transfected with GFP (Fig. 4 F, arrows). In contrast, in the dynamitin-disrupted clones, the fraction of LAT associated with intracellular compartments (Bonello et al., 2004) remained in the vicinity of the MTOC (Fig. 4 F, arrowheads). Therefore, this LAT fraction cannot contribute to the formation and maturation of the IS because the MTOC remains delocalized from it. Vav1 phosphorylated at Tyr174 did accumulate at the IS (Fig. 4 G, arrows), though to a lesser extent than in control cells, which is consistent with the low level of phosphorylation detected in the dynamitin-disrupted clones (Fig. 4 C). In contrast, PKCθ clustered at the IS in the dynamitin-disrupted clones (Fig. 4 H).

DHC silencing impairs TCR signaling

Reductions in the phosphorylation of ZAP70 (Y315), LAT (Y132), LAT (Y191), Vav1 (Y174), and downstream targets were also observed in DHC-interfered Jurkat cells (Fig. 5 A). As with the p50-dynamitin-GFP clones, phosphorylation of LAT (Y132) in DHC-interfered cells was strongly reduced. Moreover, PLCγ-1 phosphorylation at residue Y783 was also diminished. LAT phosphorylation at residues Y132, Y171, Y191, and Y226 was also strongly reduced (Fig. 5 A). Similar results were obtained in DHC-interfered CH7C17 cells stimulated either with specific HA antigenic peptide (Fig. 5 B) or with SEB (not depicted). These results establish a correlation between the failure in MTOC translocation detected in DHC-interfered cells and the decrease in LAT phosphorylation. In contrast, phosphorylation of PKCθ (T538) and Erk1/2 were not impaired, but rather occurred slightly more rapidly or were accentuated in DHC-interfered cells compared with control cells (Fig. 5 A and B), which is parallel to what occurred in dynamitin-disrupted cells (Fig. 4, D and E).

Interleukin-2 (IL-2) production is impaired in T cells by p50-dynamitin-GFP overexpression or knockdown of dynein expression

The functional effect of impaired MTOC translocation was assessed by examining T cell activation parameters. In p50-dynamitin-GFP–overexpressing cells forming conjugates with SEE-pulsed Raji APC, the expression of CD69 was not altered compared with parental T cells (not depicted) or GFP-overexpressing control clones (Fig. 6 A). But IL-2 production by the dynamitin-disrupted clones was negligible, as measured both in culture supernatants from cell conjugates and in their counterpart intracellular compartments (Fig. 6, B and C). Reduced IL-2 production was also detected in DHC-interfered cells (Fig. 6 D), which correlates with the observed decrease in MTOC translocation.

Discussion

In this study, we investigated the involvement of microtubules' minus-end motor complexes in the movement of the MTOC toward the IS. In this sense, MTOC movement and positioning has been analyzed before in relation to dynein in several functional processes, such as cell polarization and division (Vallee and Stehman, 2005; for review see Hook and Vallee, 2006). Dynein–dynactin complexes might also be important in T cell physiology because MTOC positioning during T cell activation helps proper effector functions such as cytokine secretion (Kupfer et al., 1991) and target cell killing (Kupfer and Dennert, 1984; Kupfer et al., 1985; Stinchcombe et al., 2001). We provide evidence that dynein–dynactin is functionally required

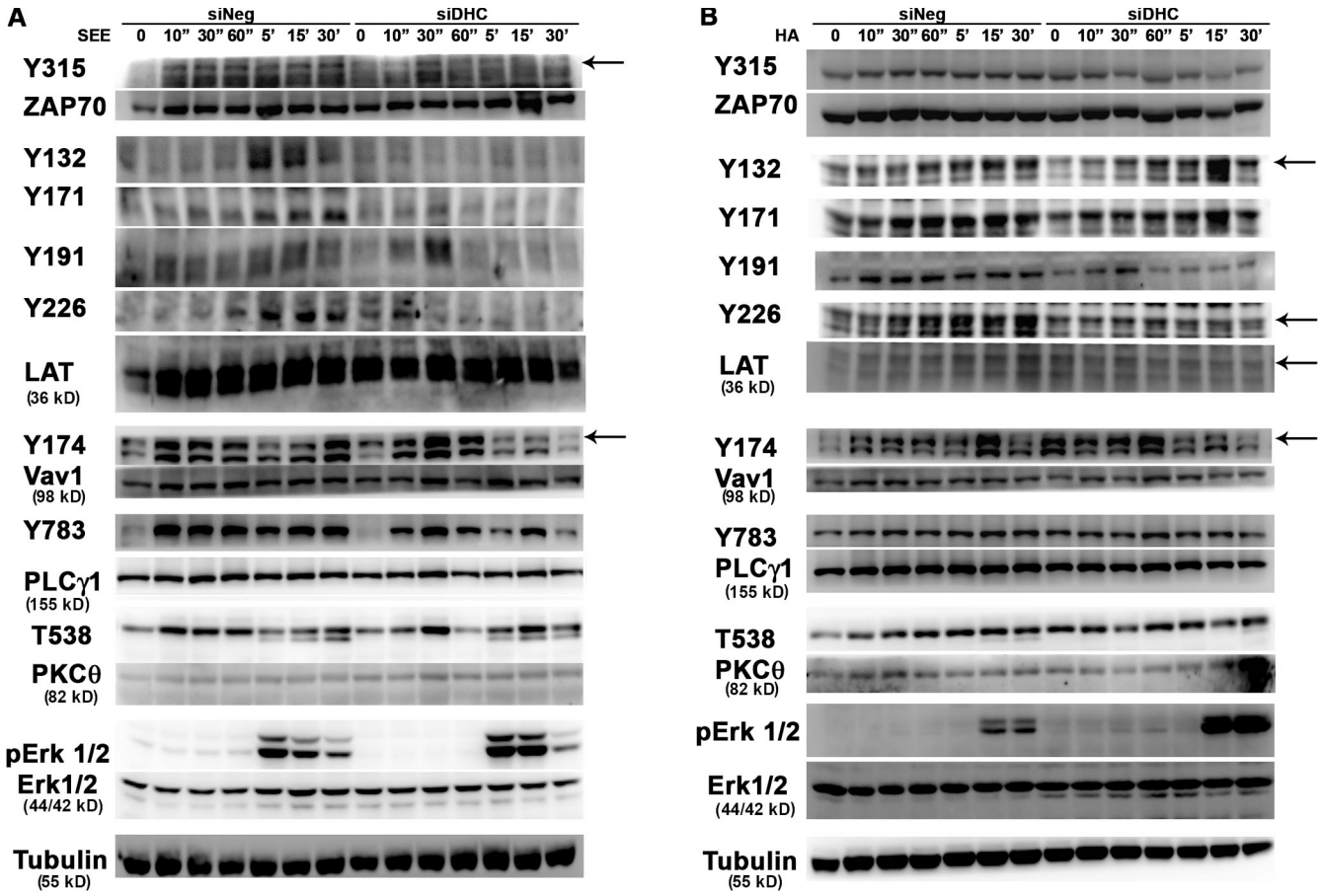

Figure 5. **TCR-sustained signaling is impaired by RNA interference of DHC (A and B) Western analysis of signaling proteins in conjugates formed for the times indicated between DHC silenced T cells (siDHC) or controls (siNeg) and activated APC.** T cell–APC pairs were J77 cells and SEE-pulsed Raji cells (0.3 µg/ml; A) and CH7C17 cells and HA peptide-preloaded Hom2 cells (50 µg/ml; B). pY783 PLCγ1, PLCγ1 phosphorylated on Y783; all other kinases are as in Fig. 4 (A–E). One out of four representative experiments is shown. Tubulin is shown as additional loading control. Arrows indicate target band sizes.

to pull microtubules so as to bring the MTOC into close apposition with the plasma membrane at the IS. To this end, we have either disrupted the dynein–dynactin complex by overexpressing p50-dynamitin-GFP or prevented its formation by silencing the expression of DHC.

Cytoplasmic dynein is a protein multicomplex that has been detected in several subcellular scenarios, including being associated with the MTOC or being bound to microtubules during the transport of varied cargoes (Vallee et al., 2004) and, more importantly for this study, at the cell cortex (Busson et al., 1998). Our finding that dynactin is involved in MTOC translocation toward the IS is relevant because the p74 dynein intermediate chain has been shown to cluster at the pSMAC, where it colocalizes with ADAP (Combs et al., 2006). However, whereas this earlier study did not describe the regulation of the dynein complex and its participation in IS formation, our current study provides compelling experimental evidence that the dynactin and dynein complexes cooperate in the relocation of the MTOC to the IS. Our results show that overexpression of p50-dynamitin-GFP prevents interaction between p74 intermediate chain and p150-glued. This in turn prevents remodeling of the complex upon SEE stimulation, resulting in defective MTOC movement and reorientation. Interestingly, overexpression of p50-dynamitin-GFP does not prevent localization of dynein and dynactin subunits at the IS but instead seems to interfere with their activity toward microtubules. Furthermore, knockdown of DHC expression, which abolished DHC accumulation at the contact site with the APC, also prevented MTOC translocation. This supports a model in which dynein–dynactin complexes dock at the cell periphery and pull on the microtubules to bring the MTOC in apposition to them. Consistently, inhibition of microtubule assembly with nocodazole has been reported to alter MTOC positioning in a manner dependent on dynein activity, and this process was additionally found to involve actomyosin contractility (Burakov et al., 2003). These observations, together with the loss of cortical dynein after cytochalasin D treatment (Busson et al., 1998), point to a role for the actomyosin cytoskeleton in MTOC positioning.

The link between ADAP/Fyb/SLAP130 and dynein intermediate chain may also represent a mechanism for docking the complex to the pSMAC at the IS (Combs et al., 2006). It is worth considering that ADAP is a well-known substrate of Fyn kinase, which is involved in TCR signal transduction (da Silva et al., 1997) and has been shown to be important for the formation of the pSMAC, LFA-1 clustering, and IL-2 production upon specific antigenic stimulation (Wang et al., 2004). We recently detected Fyn kinase activity in association with MTOC translocation toward the IS.

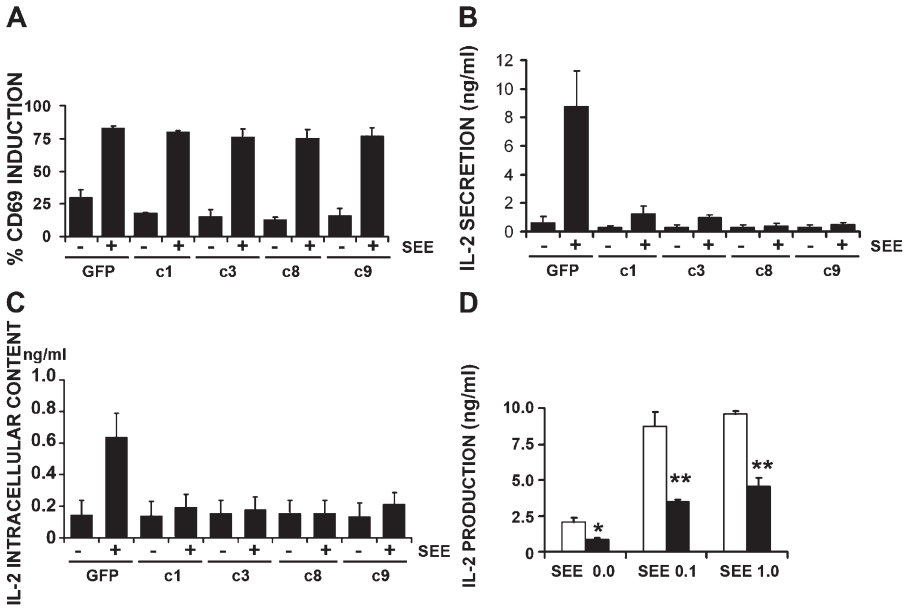

Figure 6. **IL-2 production is impaired by p50-dynamitin-GFP overexpression and DHC interference.** (A) CD69 induction was detected by flow cytometry in J77 Jurkat clones overexpressing GFP or p50-dynamitin-GFP (c) and conjugated with unprimed or SEE-pulsed Raji APC for 16 h (percentage of cells is shown). Three experiments were performed in triplicate. (B and C) IL-2 was detected by ELISA in culture supernatants (B) or cell lysates (C) from the cultures in A. Three experiments were performed in triplicate. (D) IL-2 detected by ELISA in cell supernatants from DHC-silenced J77 cells (siDHC, closed bars) and controls (siNeg, open bars) conjugated with SEE-pulsed Raji APC with the indicated doses (μg/ml). Three experiments were performed in triplicate. Data are means ± SD. *, $P < 0.05$; **, $P < 0.001$ (Student's *t* test).

Moreover, $fyn^{-/-}$ T cells were unable to translocate their MTOC toward an APC presenting antagonist peptides (Martin-Cofreces et al., 2006). This result correlates with recent evidence showing that $fyn^{-/-}$ natural killer cells are deficient in the cytolysis of target cells (Bloch-Queyrat et al., 2005), which might be a direct consequence of deficient MTOC translocation toward the IS. Fyn has been functionally linked to the tubulin cytoskeleton in neurons, where it phosphorylates Tau (Lee et al., 2004) and regulates its interaction with γ-tubulin complexes, which are involved in microtubule formation (Sulimenko et al., 2006). It is possible, therefore, that dynein–dynactin complexes act at the earliest steps of T-APC contact, where, together with ADAP and Fyn, they provide a mechanism for reorganizing the T cell tubulin cytoskeleton.

The dynamic association/dissociation of the dynein and dynactin complex upon SEE stimulation, which correlates with the observed changes in tubulin acetylation during this process (Serrador et al., 2004), may be a consequence of microtubule dynamics, supporting the role of this complex in the microtubule organization in T cells. Consistent with this idea, dynein–dynactin complexes in Jurkat cells interact with EB1 (Berrueta et al., 1999), a member of a protein family that plays a role in docking the microtubule cytoskeleton at the cell cortex, through its binding to the plus-end tips of the microtubules (Lee et al., 2000). Moreover, because the dynein–dynactin complex localizes at the pSMAC, where the microtubules are docked at the IS, it is conceivable that the molecular motor complex is pulling on the microtubules in a coordinate manner. The resulting movement would be a vectorial displacement directed to the center of the pSMAC ring, where the MTOC becomes localized as the pSMAC is structured.

We have observed that the Golgi apparatus does not translocate to the nascent IS when dynein–dynactin is inhibited and is thus dependent on microtubule minus-end motor activity. Microtubule plus-end motors (i.e., kinesins) have been shown to be dispensable for CTL killing. Inhibition of the kinesin-driven movement of lytic granules promotes their accumulation at the MTOC (the minus-end tip of the microtubules), but there are no defects in the cell killing process and MTOC translocation (Stinchcombe et al., 2006). Hence, target cell killing is absolutely dependent on MTOC/Golgi apparatus translocation to the IS, which confirms previous studies (Kupfer et al., 1985). In another study, B cell proliferation was detected only in those antigen-presenting B cells that were in close contact with the secretory area of helper T cells (Kupfer et al., 1994), which strongly supports the importance of MTOC translocation for the effector function of diverse immune cells.

Our data show that the failure of MTOC and Golgi reorientation toward the IS has important consequences for sustained TCR signaling, which is necessary for full T cell activation. This helps to explain the lack of cytokine secretion by T cells when the MTOC fails to translocate (this paper; Serrador et al., 2004). Our data thus underscore the importance of correct MTOC translocation not only for polarized secretion but also for cytokine production. This is an important finding that suggests the existence of two key regulatory checkpoints during antigenic T cell activation: (1) antigen recognition and immediate signals triggered by TCR engagement, and (2) TCR-driven MTOC translocation, which represents a positive feedback for sustained TCR signaling. Accordingly, we also observed deficiencies in Vav1 phosphorylation at Y174 in dynamitin-disrupted cells. Phosphorylation of Vav1 (Y174) is a marker of the activation of Vav1 (Lopez-Lago et al., 2000). In this regard, a correlation has been found between Fyn activation and the phosphorylation of Vav1 upon antagonist-mediated TCR activation (Huang et al., 2000), and subsequent MTOC translocation in Fyn-deficient T cells (Martin-Cofreces et al., 2006). Supporting this, the MTOC is not correctly translocated in $vav1^{-/-}$ double-positive thymocytes (Ardouin et al., 2003). Thus, the activity of Vav1 as a GEF for members of the Rho family of GTPases may be important for MTOC translocation, and might be facilitated by the reorganization of different molecular complexes at the T cell-APC contact area. Moreover, Vav1 has been shown to control both TCR-CD3

and LFA-1 clustering at the IS (Krawczyk et al., 2002). These results point to a role for dynein–dynactin complexes not only in MTOC translocation but also in the regulation of the activity of molecules important for the control of MTOC translocation throughout early TCR signaling. Together, these lines of evidence might indicate a role for the dynein–dynactin complex as a molecular platform that nucleates proteins and supplies signaling molecules to the IS. In this model, the dynein–dynactin complex would be upstream of Vav1 activation in the pathways emerging from the TCR.

The idea that dynein–dynactin complexes could act as docking sites for the relocation and delivery of regulatory and signaling proteins in T cells is attractive because these multimolecular complexes of at least 1.5 MD offer multiple domains for protein interactions (Vallee and Stehman, 2005). The dynein–dynactin complex may thus be important for the correct spatial distribution of key proteins at the IS, and our results with LFA-1 and CD3 provide evidence to support this proposal; when dynein–dynactin complexes are dissociated by dynamitin overexpression, LFA-1 does not form a clear ring at the periphery of the IS, and CD3 is distributed in multiple clusters near the peripheral ring instead of being localized at a central cluster. The altered localization of CD3 could contribute to the anomalous signaling observed in dynamitin-disrupted T cell clones or DHC-silenced cells after antigenic stimulation.

An alternative explanation might be that failed MTOC translocation could prevent the IS from adopting a proper conformation as a result of deficient activation and targeting to the IS of a second pool of signaling proteins, such as Lck, Fyn (Ley et al., 1994), or LAT (Bonello et al., 2004). It is interesting that when a nonphosphorylatable LAT mutant (Y132,191,171,226F) is expressed in LAT-deficient Jurkat cells, the intracellular LAT pool does not polarize, which demonstrates that specific phosphorylation of LAT is critical for its recruitment to the IS (Bonello et al., 2004). However, our data do not show a complete failure of LAT phosphorylation upon TCR triggering but rather a reduction in its extent. This defect could be attributed to impairment of the supply of a second wave of LAT molecules from intracellular vesicle stores to the IS. Hence, it is conceivable that there may be two waves of activation upon TCR triggering, and that failed MTOC translocation (which is normally accomplished within 2–5 min) might specifically affect the second wave. In addition, some signaling events seem to be slightly accelerated by dynein–dynactin inhibition, such as PKCθ and Erk1/2 phosphorylation. This defect may be related to the lack of correct TCR activation, which would highlight signaling through integrins. PKCθ activation would therefore be regulated by the balance between LFA-1 and the strength of TCR activation.

Our study provides mechanistic insights into the relationship between MTOC translocation and T cell activation, as measured by the activation of T cell signaling molecules and IL-2 production. There is growing evidence for the importance of MTOC translocation in this process (for reviews see Sancho et al., 2002b; Billadeau et al., 2007), e.g., in relation to LAT (Bonello et al., 2004), Fyn kinase (Martin-Cofreces et al., 2006), HDAC6 activity (Serrador et al., 2004), and, in the present study, the dynein–dynactin complex. In sum, our data support a role for the dynein–dynactin complex in regulating the signaling events that follow TCR activation, possibly by acting as a multimolecular scaffold structure that anchors at the pSMAC and plays a direct role in MTOC reorientation and recruitment to the IS.

Materials and methods

Cells and mutant constructs

Jurkat J77cl20 (J77) Vβ8 T cell clones (Niedergang et al., 1997) and the lymphoblastoid B cell lines Raji and Hom2 were cultured in complete medium (RPMI-1640 and 10% FCS; Invitrogen). CH7C17 cells (bearing a Vβ3 TCR specific for HA peptide and SEB; Hewitt et al., 1992) were cultured in complete medium supplemented with 4 μg/ml puromycin and 0.4 mg/ml hygromycin B. Culture medium for clones stably expressing GFP or p50-dynamitin-GFP was supplemented with 1 mg/ml G418. The cDNA coding for p50-dynamitin-GFP (Echeverri et al., 1996) was provided by R. Vallee (Columbia University, New York, NY).

Reagents and antibodies

The 80-kD fibronectin fragment (FN80) was a gift of A. García-Pardo (Centro de Investigaciones Biológicas, Madrid, Spain). Poly-L-lysine (PLL) and G418 were obtained from Sigma-Aldrich, and SEE was obtained from Toxin Technology. Puromycin was obtained from InvivoGen, hygromycin B was obtained from Roche, the fluorescent secondary antibodies (Alexa 568 and 647, and rhodamine red X) and cell trackers (7-amino-4-chloromethylcoumarin [CMAC], 5-(and-6)-(((4-chloromethyl)benzoyl)amino)tetramethylrhodamine [CMTMR]) were from obtained from Invitrogen, and rabbit muscle enolase was obtained from Sigma-Aldrich. All other reagents were of the purest grade available. The antibodies T3b, 448 (both anti–human-CD3), 4G10, and TP1/55 (anti–human CD69) were produced in the laboratory. Anti-phosphoVav (Y174) was a gift of X. Bustelo (Centro de Investigación del Cáncer, Salamanca, Spain). JL-8 anti-GFP, biotin-labeled anti–human V8, anti–p150-glued, anti–p50-dynamitin, and anti-Fyb/ADAP/SLAP130 monoclonal antibodies were obtained from BD Biosciences/Clontech. Unconjugated and FITC-conjugated anti–α-tubulin, anti–γ-tubulin, and anti–DHC (clone 440) were obtained from Sigma-Aldrich. Anti-Lck, anti-PKCθ (Sc-13 and Sc-18), and polyclonal goat anti-DHC were obtained from Santa Cruz Biotechnology, Inc. Anti-Vav, anti-LAT, anti–phospho-LAT (Y191 and Y226), and anti-Erk1/2, as well as anti-p74 dynein intermediate chain clone 74.1 were obtained from Millipore. Anti–phospho-LAT (Y132), anti-ZAP70, and anti–phospho-ZAP70 (Y493, Y315) were obtained from Abcam. Anti–phospho-LAT (Y171), anti–phospho-Erk1/2, anti–phospho-PLCγ-1 (Y783), anti–PLCγ-1, and anti–phospho-PKCθ (T538) were obtained from Cell Signaling Technology.

siRNA assay

Double-stranded DNC siRNA (21 bp; DYNC1H1, available from GenBank/EMBL/DDBJ under accession no. NM_001376) and the negative control were obtained from Ambion. Once we identified two oligonucleotides that knocked down the expression of the protein, a 1:1 mix of the two was used: 5′-GCACCGACAUGAUCUUCAATT-3′ and 5′-CCAGGAGUUUCGACAGUGATT-3′. 2 $\times 10^7$ Jurkat J77c20 cells were electroporated with the siRNA using the Gene Pulser II electroporation system (Bio-Rad Laboratories). Cells were cultured for 3 d and a new round of transfection was performed. Cells were used and analyzed at day six. Efficiency was assessed by Western blotting and immunofluorescence.

Cell conjugate formation, MTOC translocation, and functional assays

Raji B cells were loaded with the blue fluorescent cell tracker CMAC as described previously (Sancho et al., 2002a). Cells were then incubated for 20 min with 0.3 μg/ml SEE (or vehicle control) and washed extensively. Hom2 cells were loaded with CMAC and incubated for 2 h with 50 μg/ml HA peptide or 10 μg/ml SEB. T cells (Jurkat or CH7C17 cells, 2 $\times 10^5$ cells per slide) were mixed with an equal number of APC; the cell mixes were then centrifuged at a low speed to favor conjugate formation, gently resuspended, and plated onto slides coated with PLL (Jurkat) or fibronectin (FN; CH7C17) in humidified incubation chambers, and finally allowed to settle for 15 min at 37°C. For general analyses, PLL- or FN-adhered cells were fixed with 4% paraformaldehyde in PBS and permeabilized for 5 min in 2% paraformaldehyde and 0.2% Triton X-100 in TBS-BSA (3%). For analysis of dynein and dynactin components, cells were fixed in 4% paraformaldehyde in PHEM (60 mM Pipes, 25 mM Hepes, 5 mM EGTA, and 2mM $MgCl_2$, pH 6.9) and permeabilized in 2% paraformaldehyde and 0.2% Triton X-100 in PHEM-BSA (3%). Cell conjugates were stained with the indicated antibodies in immunofluorescence solution (50 mM Tris-HCl, pH 7.2,

150 mM NaCl, 3% BSA or PHEM, 3% BSA, and 0.2% Triton X-100 as required). Alexa 647–, Alexa 568–, and rhodamine red X–labeled highly cross-absorbed secondary antibodies were used as was appropriate (Invitrogen). Fixed cells were mounted on a mowiol-based mounting medium (ProLong Gold antifade reagent; Invitrogen) and observed at 22°C on a photomicroscope (DMR; Leica) with an HCX PL APO 63/1.32-0.6 oil objective (Leica) coupled to a COHU 4912–5010 charge-coupled device camera (Cohu; Figs. 2 and 3 A). The acquisition software was QFISH V2.1 (Leica), and images were processed with Photoshop CS (Adobe). Alternatively, cells were viewed with a TCS SP confocal laser scanning unit (Leica) attached to an inverted epifluorescence microscope (DMIRBE; Leica) with an HCX PL APO 63x/1.32-0.6 oil objective lens (Figs. 3 C and S3) or with a confocal laser scanning unit (TCS SP5; Leica) attached to an inverted epifluorescence microscope (DMI6000; Leica) with an HCX PL APO 63X/1.40-0.6 oil λ_{BL} objective. Images were acquired and processed with accompanying confocal software (LCS; Leica). 3D maximal projections of the T cell–APC contact area were produced with LCS to obtain a z stack projection. Figures were composed with Photoshop CS.

The proportion of conjugates with MTOC redistributed close to the T cell–APC contact area was calculated by random selection of >150 conjugates from at least three independent experiments. Results are expressed as the percentage of conjugates with MTOC redistributed to the contact area. CD3 distribution was used as an index of cSMAC localization without the need to permeabilize cells. Cells were analyzed by confocal microscopy, with the same conditions used for control and dynamitin-disrupted cells. 3D maximal projections were generated to produce a z stack projection of the region of cell–cell contact. The stained area was then calculated using confocal software (Leica).

For IL-2 production and CD69 expression assays, conjugates were formed as indicated above in flat-bottom 96-well plates. Supernatants were harvested after 16 h of coculture and analyzed for IL-2 production by ELISA (Diaclone). T cells from the same coculture were lysed and analyzed for intracellular IL-2 content (ELISA) or for CD69 expression using conventional double immunofluorescence techniques and flow cytometry in a FACScalibur (Becton Dickinson). Data were processed with CellQuest Pro 4.0.2 software (BD Biosciences).

Time-lapse fluorescence confocal microscopy

Raji APC (5×10^5; SEE-pulsed or controls) were allowed to adhere on FN-coated coverslips. The cells were maintained in 1 ml of HBSS (2% BSA) in Attofluor open chambers (Invitrogen) at 37°C in a 5% CO_2 atmosphere, and placed on the microscope stage. Jurkat T cells (5×10^5) were added and a series of fluorescence and differential interference contrast frames were captured simultaneously every 30 s using a TCS SP confocal laser scanning unit attached to a DMIRBE inverted epifluorescence microscope with a HCX PL APO 63x/1.32-0.60 oil objective (M1 and M3), or a TCS SP5 confocal laser scanning unit attached to an inverted epifluorescence microscope (DMI6000), with an HCX PL APO 63X/1.40-0.6 oil λ_{BL} (M2). Images were acquired and processed with the accompanying confocal software (LCS; Leica). Premiere 6.0 software (Adobe) was used for generating QuickTime videos (Apple).

Immunoprecipitation and Western blotting

For immunoprecipitation, Jurkat cells were serum starved and Raji B cells were cultured in medium containing 2% FCS for 18 h. Raji cells (5×10^6) were then preloaded with 0.3 µg/ml SEE at 37°C for 20 min and mixed with 10^8 Jurkat cells at 37°C. After incubation, cells were lysed at 4°C for 40 min in 50 mM Tris-HCl, pH 7.5, containing 1% NP-40, 0.2% Triton X-100, 150 mM NaCl, and phosphatase and protease inhibitors. Cell lysates were spun at 2,500 *g* for 10 min to remove cell debris and nuclei. Supernatants were precleared with protein G–sepharose beads at 4°C overnight and immunoprecipitated with mouse anti-p74 or anti–p150-glued for 4 h at 4°C. Protein G–sepharose beads were added for 20 min at 4°C. Immunoprecipitates were washed six times with lysis buffer and processed for Western blotting.

For Western blots and analysis of phosphorylation during T cell presentation, immunoprecipitated proteins and whole lysates (lysed as above) were analyzed by SDS-PAGE, transferred to nitrocellulose membranes, and probed with the indicated antibodies in TBS–Tween 20. Bound antibodies were reacted with HRP secondary antibodies, and proteins were visualized by enhanced chemiluminescence with SuperSignal West Pico chemiluminescent substrate (Pierce). Densitometric analyses were performed with ImageGauge 3.46 software (Fujifilm).

Online supplemental material

Fig. S1 shows that dynein–dynactin components localize at MTOC, microtubules, and cortical tubulin cytoskeleton in Jurkat T cells. Fig. S2 illustrates the generation of p50-dynamitin-GFP clones, showing a FACS profile of GFP expression in p50-dynamitin-GFP J77c120 T cell clone c1 and a Western blot of GFP in J77c120 T cell clones. Fig. S3 shows a z projection of confocal slices where Golgi translocation toward the IS is impaired in dynamitin-disrupted cells (clone c8) conjugated with SEE-pulsed Raji cells. Fig. S4 shows a confocal z slice showing that ADAP colocalizes with p50-GFP at the IS formed by the dynamitin-disrupted cells. Fig. S5 shows a confocal z projection of conjugates formed as in Fig. 1 and stained for phosphotyrosine, showing that 4G10 staining (red in merge images, labeled with Alexa 568) was not clustered at the contact area in p50-dynamitin-GFP clones as it was in GFP clones. Videos 1–3 show time-lapse confocal video microscopy showing the dynamics of MTOC movement in Jurkat T cells overexpressing paxillin-GFP (green, M1) or p50-dynamitin-GFP (green, M2 and M3) conjugated with SEE-pulsed Raji APC loaded with CMCTR cell tracker (red/orange). Supplemental videos are displayed as image sequences in Fig. 1 F at the times indicated. Online supplemental material is available at http://www.jcb.org/cgi/content/full/jcb.200801014/DC1.

We thank Dr. S. Bartlett, M. Gómez, and J. Serrador for helpful discussion and editing. We also thank Dr. R. Vallee for valuable reagents and support and Dr. M. Poenie for helpful discussion.

This study was supported by the Instituto de Salud Carlos III, Ministerio de Sanidad y Consumo, Spain (Red Temática de Investigación en Enfermedades Cardiovasculares grant RD06/0021/2006 and postdoctoral fellowship to N.B. Martín-Cófreces), Ministerio de Educación y Ciencia of Spain (grant BFU200508435/BMC and Formación Profesorado Universitario fellowship to J. Robles-Valero), Juan March Foundation (Ayuda a la Investigación Básica 2002) and grant INSINET0159/2006 from Comunidad de Madrid.

Submitted: 3 January 2008
Accepted: 14 August 2008

References

Ardouin, L., M. Bracke, A. Mathiot, S.N. Pagakis, T. Norton, N. Hogg, and V.L. Tybulewicz. 2003. Vav1 transduces TCR signals required for LFA-1 function and cell polarization at the immunological synapse. *Eur. J. Immunol.* 33:790–797.

Barreiro, O., H. de la Fuente, M. Mittelbrunn, and F. Sanchez-Madrid. 2007. Functional insights on the polarized redistribution of leukocyte integrins and their ligands during leukocyte migration and immune interactions. *Immunol. Rev.* 218:147–164.

Berrueta, L., J.S. Tirnauer, S.C. Schuyler, D. Pellman, and B.E. Bierer. 1999. The APC-associated protein EB1 associates with components of the dynactin complex and cytoplasmic dynein intermediate chain. *Curr. Biol.* 9:425–428.

Billadeau, D.D., J.C. Nolz, and T.S. Gomez. 2007. Regulation of T-cell activation by the cytoskeleton. *Nat. Rev. Immunol.* 7:131–143.

Blanchard, N., V. Di Bartolo, and C. Hivroz. 2002. In the immune synapse, ZAP-70 controls T cell polarization and recruitment of signaling proteins but not formation of the synaptic pattern. *Immunity.* 17:389–399.

Bloch-Queyrat, C., M.C. Fondaneche, R. Chen, L. Yin, F. Relouzat, A. Veillette, A. Fischer, and S. Latour. 2005. Regulation of natural cytotoxicity by the adaptor SAP and the Src-related kinase Fyn. *J. Exp. Med.* 202:181–192.

Bonello, G., N. Blanchard, M.C. Montoya, E. Aguado, C. Langlet, H.T. He, S. Nunez-Cruz, M. Malissen, F. Sanchez-Madrid, D. Olive, et al. 2004. Dynamic recruitment of the adaptor protein LAT: LAT exists in two distinct intracellular pools and controls its own recruitment. *J. Cell Sci.* 117:1009–1016.

Burakov, A., E. Nadezhdina, B. Slepchenko, and V. Rodionov. 2003. Centrosome positioning in interphase cells. *J. Cell Biol.* 162:963–969.

Busson, S., D. Dujardin, A. Moreau, J. Dompierre, and J.R. De Mey. 1998. Dynein and dynactin are localized to astral microtubules and at cortical sites in mitotic epithelial cells. *Curr. Biol.* 8:541–544.

Combs, J., S.J. Kim, S. Tan, L.A. Ligon, E.L. Holzbaur, J. Kuhn, and M. Poenie. 2006. Recruitment of dynein to the Jurkat immunological synapse. *Proc. Natl. Acad. Sci. USA.* 103:14883–14888.

Das, V., B. Nal, A. Roumier, V. Meas-Yedid, C. Zimmer, J.C. Olivo-Marin, P. Roux, P. Ferrier, A. Dautry-Varsat, and A. Alcover. 2002. Membrane-cytoskeleton interactions during the formation of the immunological synapse and subsequent T-cell activation. *Immunol. Rev.* 189:123–135.

da Silva, A.J., Z. Li, C. de Vera, E. Canto, P. Findell, and C.E. Rudd. 1997. Cloning of a novel T-cell protein FYB that binds FYN and SH2-domain-containing leukocyte protein 76 and modulates interleukin 2 production. *Proc. Natl. Acad. Sci. USA.* 94:7493–7498.

Dustin, M.L., M.W. Olszowy, A.D. Holdorf, J. Li, S. Bromley, N. Desai, P. Widder, F. Rosenberger, P.A. van der Merwe, P.M. Allen, and A.S. Shaw. 1998. A novel adaptor protein orchestrates receptor patterning and cytoskeletal polarity in T-cell contacts. *Cell.* 94:667–677.

Echeverri, C.J., B.M. Paschal, K.T. Vaughan, and R.B. Vallee. 1996. Molecular characterization of the 50-kD subunit of dynactin reveals function for the complex in chromosome alignment and spindle organization during mitosis. *J. Cell Biol.* 132:617–633.

Grakoui, A., S.K. Bromley, C. Sumen, M.M. Davis, A.S. Shaw, P.M. Allen, and M.L. Dustin. 1999. The immunological synapse: a molecular machine controlling T cell activation. *Science.* 285:221–227.

Grieshaber, S.S., N.A. Grieshaber, and T. Hackstadt. 2003. *Chlamydia trachomatis* uses host cell dynein to traffic to the microtubule-organizing center in a p50 dynamitin-independent process. *J. Cell Sci.* 116:3793–3802.

Herreros, L., J.L. Rodriguez-Fernandez, M.C. Brown, J.L. Alonso-Lebrero, C. Cabanas, F. Sanchez-Madrid, N. Longo, C.E. Turner, and P. Sanchez-Mateos. 2000. Paxillin localizes to the lymphocyte microtubule organizing center and associates with the microtubule cytoskeleton. *J. Biol. Chem.* 275:26436–26440.

Hewitt, C.R., J.R. Lamb, J. Hayball, M. Hill, M.J. Owenm, and R.E. O'Heir. 1992. Major histocompatibility complex independent clonal T cell anergy by direct interaction of *Staphyloccocus aureus* enterotoxin B with the T cell antigen receptor. *J. Exp. Med.* 175:1493–1499.

Hirokawa, N. 1998. Kinesin and dynein superfamily proteins and the mechanism of organelle transport. *Science.* 279:519–526.

Hook, P., and R.B. Vallee. 2006. The dynein family at a glance. *J. Cell Sci.* 119:4369–4371.

Houtman, J.C., R.A. Houghtling, M. Barda-Saad, Y. Toda, and L.E. Samelson. 2005. Early phosphorylation kinetics of proteins involved in proximal TCR-mediated signaling pathways. *J. Immunol.* 175:2449–2458.

Huang, J., D. Tilly, A. Altman, K. Sugie, and H.M. Grey. 2000. T-cell receptor antagonists induce Vav phosphorylation by selective activation of Fyn kinase. *Proc. Natl. Acad. Sci. USA.* 97:10923–10929.

King, S.J., C.L. Brown, K.C. Maier, N.J. Quintyne, and T.A. Schroer. 2003. Analysis of the dynein-dynactin interaction in vitro and in vivo. *Mol. Biol. Cell.* 14:5089–5097.

Krawczyk, C., A. Oliveira-dos-Santos, T. Sasaki, E. Griffiths, P.S. Ohashi, S. Snapper, F. Alt, and J.M. Penninger. 2002. Vav1 controls integrin clustering and MHC/peptide-specific cell adhesion to antigen-presenting cells. *Immunity.* 16:331–343.

Kupfer, A., and G. Dennert. 1984. Reorientation of the microtubule-organizing center and the Golgi apparatus in cloned cytotoxic lymphocytes triggered by binding to lysable target cells. *J. Immunol.* 133:2762–2766.

Kupfer, A., and S.J. Singer. 1989. The specific interaction of helper T cells and antigen-presenting B cells. IV. Membrane and cytoskeletal reorganizations in the bound T cell as a function of antigen dose. *J. Exp. Med.* 170:1697–1713.

Kupfer, A., G. Dennert, and S.J. Singer. 1985. The reorientation of the Golgi apparatus and the microtubule-organizing center in the cytotoxic effector cell is a prerequisite in the lysis of bound target cells. *J. Mol. Cell. Immunol.* 2:37–49.

Kupfer, A., S.L. Swain, and S.J. Singer. 1987. The specific direct interaction of helper T cells and antigen-presenting B cells. II. Reorientation of the microtubule organizing center and reorganization of the membrane-associated cytoskeleton inside the bound helper T cells. *J. Exp. Med.* 165:1565–1580.

Kupfer, A., T.R. Mosmann, and H. Kupfer. 1991. Polarized expression of cytokines in cell conjugates of helper T cells and splenic B cells. *Proc. Natl. Acad. Sci. USA.* 88:775–779.

Kupfer, H., C.R. Monks, and A. Kupfer. 1994. Small splenic B cells that bind to antigen-specific T helper (Th) cells and face the site of cytokine production in the Th cells selectively proliferate: immunofluorescence microscopic studies of Th-B antigen-presenting cell interactions. *J. Exp. Med.* 179:1507–1515.

Lee, K.H., A.R. Dinner, C. Tu, G. Campi, S. Raychaudhuri, R. Varma, T.N. Sims, W.R. Burack, H. Wu, J. Wang, et al. 2003. The immunological synapse balances T cell receptor signaling and degradation. *Science.* 302:1218–1222.

Lee, G., R. Thangavel, V.M. Sharma, J.M. Litersky, K. Bhaskar, S.M. Fang, L.H. Do, A. Andreadis, G. Van Hoesen, and H. Ksiezak-Reding. 2004. Phosphorylation of tau by fyn: implications for Alzheimer's disease. *J. Neurosci.* 24:2304–2312.

Lee, L., J.S. Tirnauer, J. Li, S.C. Schuyler, J.Y. Liu, and D. Pellman. 2000. Positioning of the mitotic spindle by a cortical-microtubule capture mechanism. *Science.* 287:2260–2262.

Ley, S.C., M. Marsh, C.R. Bebbington, K. Proudfoot, and P. Jordan. 1994. Distinct intracellular localization of Lck and Fyn protein tyrosine kinases in human T lymphocytes. *J. Cell Biol.* 125:639–649.

Lopez-Lago, M., H. Lee, C. Cruz, N. Movilla, and X.R. Bustelo. 2000. Tyrosine phosphorylation mediates both activation and downmodulation of the biological activity of Vav. *Mol. Cell. Biol.* 20:1678–1691.

Lowin-Kropf, B., V.S. Shapiro, and A. Weiss. 1998. Cytoskeletal polarization of T cells is regulated by an immunoreceptor tyrosine-based activation motif-dependent mechanism. *J. Cell Biol.* 140:861–871.

Martin-Cofreces, N.B., D. Sancho, E. Fernandez, M. Vicente-Manzanares, M. Gordon-Alonso, M.C. Montoya, F. Michel, O. Acuto, B. Alarcon, and F. Sanchez-Madrid. 2006. Role of Fyn in the rearrangement of tubulin cytoskeleton induced through TCR. *J. Immunol.* 176:4201–4207.

Melkonian, K.A., K.C. Maier, J.E. Godfrey, M. Rodgers, and T.A. Schroer. 2007. Mechanism of dynamitin-mediated disruption of dynactin. *J. Biol. Chem.* 282:19355–19364.

Monks, C.R., B.A. Freiberg, H. Kupfer, N. Sciaky, and A. Kupfer. 1998. Three-dimensional segregation of supramolecular activation clusters in T cells. *Nature.* 395:82–86.

Niedergang, F., A. Dautry-Varsat, and A. Alcover. 1997. Peptide antigen or superantigen-induced down regulation of TCR involves both stimulated and unstimulated receptors. *J. Immunol.* 159:1703–1710.

Palazzo, A.F., H.L. Joseph, Y.J. Chen, D.L. Dujardin, A.S. Alberts, K.K. Pfister, R.B. Vallee, and G.G. Gundersen. 2001. Cdc42, dynein, and dynactin regulate MTOC reorientation independent of Rho-regulated microtubule stabilization. *Curr. Biol.* 11:1536–1541.

Paz, P.E., S. Wang, H. Clarke, X. Lu, D. Stokoe, and A. Abo. 2001. Mapping the Zap-70 phosphorylation sites on LAT (linker for activation of T cells) required for recruitment and activation of signalling proteins in T cells. *Biochem. J.* 356:461–471.

Ross, J.L., K. Wallace, H. Shuman, Y.E. Goldman, and E.L. Holzbaur. 2006. Processive bidirectional motion of dynein-dynactin complexes in vitro. *Nat. Cell Biol.* 8:562–570.

Ryser, J.E., E. Rungger-Brandle, C. Chaponnier, G. Gabbiani, and P. Vassalli. 1982. The area of attachment of cytotoxic T lymphocytes to their target cells shows high motility and polarization of actin, but not myosin. *J. Immunol.* 128:1159–1162.

Sancho, D., M.C. Montoya, A. Monjas, M. Gordon-Alonso, T. Katagiri, D. Gil, R. Tejedor, B. Alarcon, and F. Sanchez-Madrid. 2002a. TCR engagement induces proline-rich tyrosine kinase-2 (Pyk2) translocation to the T Cell-APC interface independently of Pyk2 activity and in an immunoreceptor tyrosine-based activation motif-mediated fashion. *J. Immunol.* 169:292–300.

Sancho, D., M. Vicente-Manzanares, M. Mittelbrunn, M.C. Montoya, M. Gordon-Alonso, J.M. Serrador, and F. Sanchez-Madrid. 2002b. Regulation of microtubule-organizing center orientation and actomyosin cytoskeleton rearrangement during immune interactions. *Immunol. Rev.* 189:84–97.

Sedwick, C.E., M. Morgan, L. Jusino, J.L. Cannon, J. Miller, and J.K. Burkhardt. 1999. TCR, LFA-1, and CD28 play unique and complementary roles in signaling T cell cytoskeletal reorganization. *J. Immunol.* 162:1367–1375.

Serrador, J.M., J.R. Cabrero, D. Sancho, M. Mittelbrunn, A. Urzainqui, and F. Sanchez-Madrid. 2004. HDAC6 deacetylase activity links the tubulin cytoskeleton with immune synapse organization. *Immunity.* 20:417–428.

Stinchcombe, J.C., G. Bossi, S. Booth, and G.M. Griffiths. 2001. The immunological synapse of CTL contains a secretory domain and membrane bridges. *Immunity.* 15:751–761.

Stinchcombe, J.C., E. Majorovits, G. Bossi, S. Fuller, and G.M. Griffiths. 2006. Centrosome polarization delivers secretory granules to the immunological synapse. *Nature.* 443:462–465.

Sulimenko, V., E. Draberova, T. Sulimenko, L. Macurek, V. Richterova, and P. Draber. 2006. Regulation of microtubule formation in activated mast cells by complexes of gamma-tubulin with Fyn and Syk kinases. *J. Immunol.* 176:7243–7253.

Vallee, R.B., and S.A. Stehman. 2005. How dynein helps the cell find its center: a servomechanical model. *Trends Cell Biol.* 15:288–294.

Vallee, R.B., J.C. Williams, D. Varma, and L.E. Barnhart. 2004. Dynein: An ancient motor protein involved in multiple modes of transport. *J. Neurobiol.* 58:189–200.

Vaughan, K.T. 2005. Microtubule plus ends, motors, and traffic of Golgi membranes. *Biochim. Biophys. Acta.* 1744:316–324.

Vaughan, K.T., and R.B. Vallee. 1995. Cytoplasmic dynein binds dynactin through a direct interaction between the intermediate chains and p150Glued. *J. Cell Biol.* 131:1507–1516.

Vicente-Manzanares, M., and F. Sanchez-Madrid. 2004. Role of the cytoskeleton during leukocyte responses. *Nat. Rev. Immunol.* 4:110–122.

Wang, H., F.E. McCann, J.D. Gordan, X. Wu, M. Raab, T.H. Malik, D.M. Davis, and C.E. Rudd. 2004. ADAP-SLP-76 binding differentially regulates supramolecular activation cluster (SMAC) formation relative to T cell-APC conjugation. *J. Exp. Med.* 200:1063–1074.

Wu, J., Q. Zhao, T. Kurosaki, and A. Weiss. 1997. The Vav binding site (Y315) in ZAP-70 is critical for antigen receptor-mediated signal transduction. *J. Exp. Med.* 185:1877–1882.